Paleobiology, 48(1), 2022, pp. 154–170
DOI: 10.1017/pab.2021.30

PALEOBIOLOGY
A PUBLICATION OF THE Paleontological SOCIETY

Article

The taphonomic clock in fish otoliths

*Konstantina Agiadi**, *Michele Azzarone*, *Quan Hua*, *Darrell S. Kaufman*, *Danae Thivaiou*, *and Paolo G. Albano*

Abstract.—Paleobiological and paleoecological interpretations rely on constraining the temporal resolution of the fossil record. The taphonomic clock, that is, a correlation between the alteration of skeletal material and its age, is an approach for quantifying time-averaging scales. We test the taphonomic clock hypothesis for marine demersal and pelagic fish otoliths from a 10–40 m depth transect on the Mediterranean siliciclastic Israeli shelf by radiocarbon dating and taphonomic scoring. Otolith ages span the last ~8000 yr, with considerable variation in median and range along the transect. Severely altered otoliths, contrary to pristine otoliths, are likely to be older than 1000 yr. For pelagic fish otoliths, at 30 m depth, taphonomic degradation correlates positively with postmortem age. In contrast, no correlation occurs for demersal fishes at 10 and 30 m depth, mostly because of the paucity of very young pristine (<150 yr) otoliths, possibly due to a drop in production over the last few centuries. Contrary to molluscan and brachiopod shells, young otoliths at these depths are little affected and do not show a broad spectrum of taphonomic damage, because those that derive from predation are excreted in calcium- and phosphate-rich feces forming an insoluble crystallic matrix that increases their preservation potential. At 40 m depth, all dated otoliths are very young but rather damaged because of locally chemically aggressive sediments, thus showing no correlation between taphonomic grade and postmortem age. Our results show that local conditions and the target species population dynamics must be considered when testing the taphonomic clock hypothesis.

Konstantina Agiadi, Michele Azzarone, and Paolo G. Albano†. Department of Palaeontology, University of Vienna, Althanstrasse 14, A-1090, Vienna, Austria. E-mail: konstantina.agiadi@univie.ac.at, michele.azzarone2@unibo.it.
†Present address: Stazione Zoologica Anton Dohrn, Villa Comunale, 80121 Naples, Italy. E-mail: pgalbano@gmail.com

Quan Hua. Australian Nuclear Science and Technology Organisation, Kirrawee DC, NSW 2232, Australia. E-mail: qhx@ansto.gov.au

Darrell S. Kaufman. School of Earth and Sustainability, Northern Arizona University, Flagstaff, Arizona 86011, U.S.A. E-mail: Darrell.Kaufman@nau.edu

Danae Thivaiou. Department of Historical Geology and Paleontology, Faculty of Geology and Geoenvironment, National and Kapodistrian University of Athens, Panepistimioupolis 15784, Athens, Greece. E-mail: dthivaiou@geol.uoa.gr

Accepted: 30 July 2021
*Corresponding author.

Introduction

The extent of time averaging in death and fossil assemblages is crucial for quantifying the temporal resolution of the fossil record. One approach to quantify scales of time averaging is the taphonomic clock: older skeletons show a higher degree of alteration because of the accrual of skeletal damage with increasing postmortem age (Powell and Davies 1990; Kidwell 1993). The taphonomic clock is useful for unmixing assemblages into cohorts of different ages (Albano and Sabelli 2011; Belanger 2011; Yanes 2012; Hassan et al. 2014; Tomašových et al. 2017).

Experimental approaches as well as increasingly affordable geochronological tools, including radiocarbon-calibrated amino acid racemization (Allen et al. 2013) and rapid radiocarbon dating (Bush et al. 2013), have allowed researchers to test rigorously the taphonomic clock hypothesis by attempting to correlate the preservation state with postmortem age in modern to Holocene assemblages. At very short timescales, years to a few decades, the taphonomic clock works predictably: skeletal shell degradation is significantly influenced by elapsed time-since-death (e.g., Callender et al. 1994, 2002; Powell et al.

© The Author(s), 2021. Published by Cambridge University Press on behalf of The Paleontological Society. 0094-8373/22

https://doi.org/10.1017/pab.2021.30 Published online by Cambridge University Press

2002, 2008, 2011; Klompmaker et al. 2017; Cristini and De Francesco 2019). In the longest experiment on molluscan shells, which lasted 13 yr, edge alteration showed the most dramatic increases with time, and most shells were discolored after just 2 yr (Powell et al. 2011). Over timescales from decades to millennia, correlative studies gave less straightforward results: heavily damaged shells are generally old, but young shells can also appear old and old shells can be well preserved (Powell and Davies 1990; Flessa et al. 1993; Kowalewski et al. 1994; Martin et al. 1996; Kidwell 1998; Carroll et al. 2003; Kidwell et al. 2005). When it comes to individual alteration variables, Powell and Davies (1990) found that only shell color could be used to confidently separate old from young beached *Donax* bivalve shells, which was confirmed with experimental results by Powell et al. (2011). Similarly, Kowalewski et al. (1994) found correlation only between bivalve shell luster and postmortem age when comparing shelly cheniers of ages spanning 70 to 5000 yr; other taphonomic variables did not present significant correlations. Studying venerid bivalves, Flessa et al. (1993) found a moderately positive correlation between preservation state and postmortem age on tidal flats in Mexico and reported that the bivalve shell surface was modified early in taphonomic history, whereas material loss took place later on. Over even longer timescales, the taphonomic clock works unambiguously: Pleistocene shells can be consistently distinguished from modern shells (Frey and Howard 1986; Henderson and Frey 1986; Flessa 1993; Yanes 2012), suggesting that the taphonomic clock is sensitive to age differences in the $>10^4$ yr range (Frey and Howard 1986; Kidwell 1993; Wehmiller et al. 1995).

The apparent inconsistency in the relationship between damage and age over different timescales can be reconciled, considering that such results derive from the two-phase process of taphonomic loss in surficial sediments (Tomašových et al. 2014, 2016). First, degradation of skeletal material occurs quickly in the taphonomically active zone (TAZ), so that even young skeletons may accrue significant damage (Carroll et al. 2003)—results consistent with the strong correlation observed in experiments. Then, upon burial, skeletal loss slows down in the sequestration zone (SZ) because of greater protection from most drivers of alteration. These skeletons occasionally return to the TAZ, for example, as a result of bioturbation, contributing to the long tail of old skeletons often observed in the age–frequency distributions of surficial assemblages (e.g., Kowalewski et al. 1998; Carroll et al. 2003; Harnik et al. 2017; Ritter et al. 2017; Tomašových and Kidwell 2017; Albano et al. 2020). The processes of destruction and burial are stochastic (Olszewski 2004). A skeleton can be buried quickly, thus avoiding significant degradation, and be re-exhumed much later, contributing old shells in good preservation state, as observed empirically. In contrast, a skeleton may remain at the sediment–water interface longer, accruing significant damage in a relatively short period of time. Therefore, correlative studies on skeletons decades to millennia old may provide noisy data and show only moderate correlations. However, over very long timescales, even the more conservative taphonomic features show a consistent trend of degradation with age.

The taphonomic clock proves useful in both ecologic and paleontological applications. The rapid loss of luster in shells enables discriminating fresh dead specimens from older ones; such fresh shells can be added to counts of living individuals, for example, to overcome the low detectability of most land snails (Cernohorsky et al. 2010; Albano 2014). Additionally, even though geochronological methods can nowadays routinely be used to quantify time averaging in the Holocene, they are destructive methods. Despite continuous improvements that now enable dating samples with less than 1 mg mass (Bush et al. 2013; Gottschalk et al. 2018; Bright et al. 2021), whole small skeletons may be required, conflicting with other research needs.

A major example of such small skeletal parts is fish otoliths. They are incremental structures in the inner ear of marine fishes that facilitate sound and balance perception (Schulz-Mirbach et al. 2018). Due to their species-specific morphology, sagittal otoliths, which are aragonitic (Degens et al. 1969), are valuable for reconstructing past fish faunas. Establishing the taphonomic clock of otoliths is important,

https://doi.org/10.1017/pab.2021.30 Published online by Cambridge University Press

because marine fish otoliths are commonly used for studying fish evolutionary patterns (e.g., Landini and Sorbini 2005), fish paleobiogeography (e.g., Girone et al. 2006; Agiadi et al. 2011, 2017, 2018; Aguilera et al. 2014; Schwarzhans et al. 2020), and paleoenvironmental conditions, including paleoclimate and paleodepth (Andrus et al. 2002; Girone 2005; Price et al. 2009; Agiadi et al. 2010, 2020; Bertucci et al. 2018; Jones and Checkley 2019; Sandweiss et al. 2020).

Studies on the taphonomy of otoliths are scarce (Lin et al. 2019), and the taphonomic clock has never been tested for these important vertebrate skeletal elements. We here taphonomically scored and radiocarbon-dated otoliths from a depth gradient encompassing different grain sizes on a siliciclastic shallow shelf in the eastern Mediterranean to test the hypothesis that the accrual of damage correlates with postmortem age. In addition, we compared the results for the otoliths of anchovies with those of gobies and congrids, taxa with different lifestyles, to explore the role of these factors in otolith preservation.

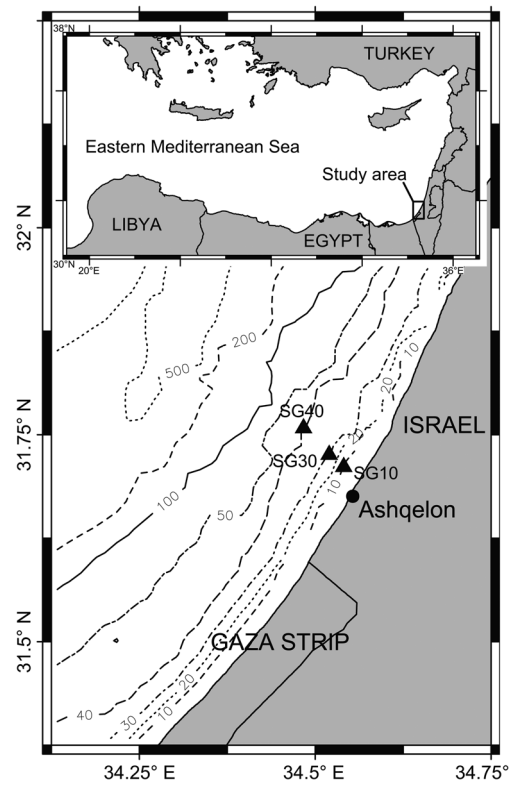


FIGURE 1. Location of the sampling stations off Ashqelon in southern Israel, Mediterranean Sea.

Materials and Methods

Study Area and Sampling.—The study area is the Mediterranean coast of southern Israel off Ashqelon (Fig. 1), which is an open shelf receiving sediment input from the Nile (Inman and Jenkins 1984). The deposition of fine-grained sediment is limited above ~35 m depth by strong wave-induced counterclockwise currents from the Nile delta northward along the Israeli coast (Golik 1993; Avnaim-Katav et al. 2015). The fair-weather wave base is located at 15–25 m depth (Hyams-Kaphzan et al. 2008). We collected sediment samples using a Van Veen grab (36.5 × 31.8 cm) onboard the RV *Mediterranean Explorer* at 10, 30, and 40 m depths (Supplementary Table S1) in autumn 2016. At each depth, we collected five replicate grab samples, sieved them with a 0.5-mm mesh, and picked otoliths from all of them to maximize sample size. The grab samples captured the first 5–20 cm of sediment, depending on grain size, which correspond to the TAZ. The sedimentation rate varies strongly along the transect, from 0.4 mm/yr and 0.2 mm/yr at 10 and 30 m depths, respectively, to 2.4 mm/yr at 40 m (Goodman-Tchernov et al. 2009; Albano et al. 2020).

Otolith Specimens.—We scored and dated 77 otoliths of two groups of fishes: pelagic fishes that occupy the higher part of the water column and travel some distance on a daily basis, specifically the codlet *Bregmaceros nectabanus* and the anchovy *Engraulis encrasicolus* ($n = 25$); and demersal fishes that live in/near the sea bottom and do not migrate, namely the congrid *Ariosoma balearicum* and the gobies *Gobius paganellus*, *Gobius auratus*, *Gobius cobitis*, *Gobius niger*, *Lesueurigobius friesii*, and *Lesueurigobius suerii* ($n = 52$). These two groups of fishes have otoliths with different shapes, thin and elongate in anchovies and thick and square/oval-shaped in gobies and congrids. Because predation may be relevant to otolith preservation and input to the seafloor (as is explained in the "Discussion"), we note that anchovies are preyed upon by pelagic and demersal

https://doi.org/10.1017/pab.2021.30 Published online by Cambridge University Press

fishes, gobies by larger pelagic and demersal fishes, and congrids by large pelagic fishes and seabirds. The studied material is shown in the Supplementary Table S2. The selection of otoliths was random, from the subset of those larger than 0.5 mg in mass, in order to achieve radiocarbon dating. In the case of *B. nectabanus*, we dated both otoliths found at the 40 m station. All stations contained otoliths of both pelagic and demersal fishes (Agiadi and Albano 2020), but we dated anchovy otoliths only from the 30 m station, because they were most abundant there.

Taphonomic Scoring Protocol.—We evaluated the preservation of the inner face of the otoliths based on six alteration variables: completeness, translucency, bioerosion, edge preservation, dissolution, and ornamentation loss. All variables were scored on a scale from 0 to 3, where 0 indicated a pristine otolith (zero damage) and 3 a strongly altered otolith (maximum damage) (Fig. 2, Table 1). Completeness reflects the level of fragmentation of the otolith. Translucency varies from almost fully translucent in pristine otoliths, to white semi-translucent and white–yellowish and opaque in very altered otoliths. Bioerosion qualitatively measures the area of the otolith affected by microborers (mainly algae, fungi, and sponges). Edge preservation measures the degree of preservation of the edge profile of the otolith, in terms of erosion or chipping. Dissolution reflects the alteration of the otolith as expressed by chalky or grainy appearance and dense pitting of the surface. Ornamentation loss indicates the preservation status of the inner-face morphology of the otolith, specifically the morphology of the sulcus acusticus and the dorsal/ventral cristae (if present in the target species originally). The complete taphonomic scoring results are reported in Supplementary Table S2.

Radiocarbon Dating.—The 77 dated otoliths belong to nine fish species. Of these, 75 were dated by accelerator mass spectrometry (AMS) radiocarbon, using powdered carbonate targets following the methodology of Bush et al. (2013). They were prepared at the Northern Arizona University and measured at the University of California at Irvine. The two otoliths of *B. nectabanus* were dated using the gas-ion source of the MICADAS AMS at the University of Bern, as described by Gottschalk et al. (2018). The calibrated radiocarbon ages (Supplementary Table S2) were expressed in calendar years before 2016 (year of collecting). Details of the radiocarbon and calibration procedures are available in the Supplementary Material.

Data Analysis.—We described the age–frequency distributions of the otoliths based on their range and median, and we computed Kolmogorov-Smirnov and Wilcoxon tests to compare their shapes and medians, respectively. To investigate the overall preservation state of the otoliths, we described taphonomic damage with a univariate descriptor obtained by averaging the scores of all taphonomic variables and defined four grades: pristine (0–0.5), moderate (0.5–1.5), severe (1.5–2.5), and high (2.5–3.0). We plotted the distribution of ages in relation to this univariate score with box plots and scatter plots, and then the distribution of the univariate score in relation to the sampling site. We tested for differences among groups with the Kruskal-Wallis analysis of variance and permutational multivariate analysis of variance (PERMANOVA). Pairwise *p*-values were assessed with the Holm-Bonferroni correction. In addition, we plotted the range of ages for each of the taphonomic variables and tested for correlation with the Spearman rank correlation coefficient.

We then performed principal coordinate analysis (PCoA) on all the taphonomic variables to explore variation in multivariate alteration among the otoliths, using Manhattan distances. The distribution of the otoliths (distances among specimens in the PCoA ordination space) reflected their differences in multivariate alteration that are independent of their ages. In addition, to identify the taphonomic variables that most affected the order of the specimens along the first two PCoA axes, each alteration variable was represented as a vector, produced by maximizing the correlation between the scores of the alteration variables on each individual otolith and the corresponding ordination scores along each of the first two axes using the *envfit* function of the vegan package (Oksanen et al. 2015). Each vector had two components: the direction, which reflected the highest rate of change in the score of a given

https://doi.org/10.1017/pab.2021.30 Published online by Cambridge University Press

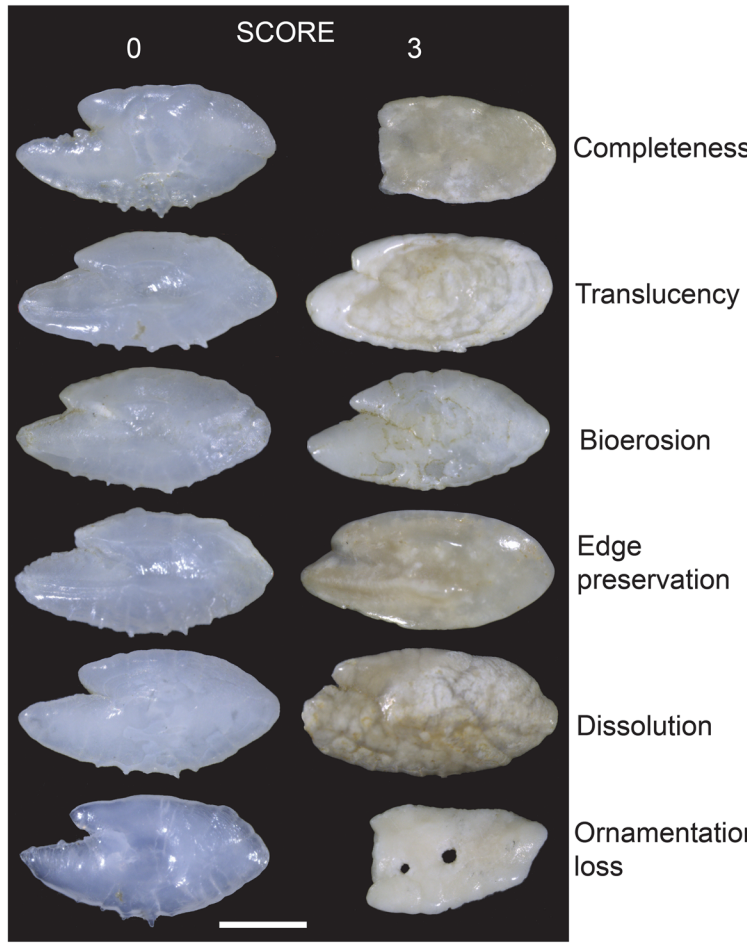


FIGURE 2. Otoliths of the anchovy *Engraulis encrasicolus* showing different degrees of degradation ranging from 0 (pristine) to 3 (heavily degraded), details given in Table 1. The otolith specimens shown are from top to bottom: OT175, OT104, OT112, OT192, OT174, and OT135 in the first column; OT181, OT101, OT136, OT183, OT109, and OT218 in the second column (full scores in Supplementary Table S3). Scale bar, 0.5 mm.

taphonomic variable (from pristine to significantly altered), and the length. The latter was scaled by correlating it with the first two ordination axes. Thus, variables with longer vectors were more strongly correlated with ordination axes. We also measured the correlation between the first ordination axis and age and between the first ordination axis and the taphonomic variables with the Spearman rank correlation coefficient. Finally, we tested the effects of age and water depth on multivariate alteration with constrained analysis of principal coordinates (CAP; Anderson and Willis 2003).

The analyses were performed for the whole dataset, for each depth, and for demersal versus pelagic species at 30 m depth, as this was the only station from which we dated large subsets of otoliths belonging to both groups. All statistical analyses were performed using R software v. 3.6.1 (R Development Core Team 2019).

Results

Age–Frequency Distributions.—The otolith assemblage spans much of the Holocene with a range of 4–7961 yr and a median of 559 yr ($n = 77$). The age ranges are markedly different at the three sites (Fig. 3). The dated otoliths are 144–1622 yr old (median = 561 yr, $n = 20$), 6–7961 yr old (median = 735 yr, $n = 47$), and

https://doi.org/10.1017/pab.2021.30 Published online by Cambridge University Press

TABLE 1. Taphonomic variables and scoring. The higher the value, the greater the taphonomic alteration.

Taphonomic variable	Possible values			
Completeness	0 = 95%–100% complete	1 = 75%–95% complete	2 = 50%–75% complete	3 = 25%–50% complete
Translucency	0 = clear, translucent	1 = white, translucent	2 = white, not translucent	3 = yellow, not translucent
Bioerosion	0 = no bioerosion	1 = 1/3 bioeroded	2 = 2/3 bioeroded	3 = more than 2/3 bioeroded
Edge preservation	0 = sharp, pristine	1 = 1/3 eroded/chipped	2 = 2/3 eroded/chipped	3 = more than 2/3 eroded/chipped
Dissolution	0 = absent	1 = patchy dissolution	2 = diffuse dissolution	3 = pervasive dissolution
Ornamentation loss	0 = pristine ornamentation	1 = ornamentation mostly preserved (>50%) but worn	2 = ornamentation traces (<50% preserved)	3 = massive loss (original ornamentation mostly erased)

4–174 yr old (median = 8 yr, $n = 10$) at 10, 30, and 40 m, respectively. At the 30 m depth, the demersal species' ($n = 22$) range is 6–4950 yr with a median of 744 yr, whereas the pelagic species' ($n = 25$) range is 11–7961 yr old with a median of 678 yr; neither the shape of the age–frequency distributions nor the medians of these two groups differ (shape: Kolmogorov-Smirnov, $D = 0.23$, $p = 0.54$; median: Wilcoxon $W = 305.5$, $p = 0.52$). Time averaging, the temporal mixing of the otolith death assemblage, expressed in terms of interquartile range is 156, 1499, and 18 yr at 10, 30, and 40 m, respectively.

Relationship between Postmortem Age and Mean Univariate Preservation.—The median of the univariate mean taphonomic grade does not differ among the stations (Kruskal Wallis test, $\chi^2 = 2.07$, $p = 0.35$; Fig. 4), but the station at 40 m (median age = 8 yr) is characterized by a lack of otoliths in pristine condition, a remarkable result considering the very young age of the assemblage.

For the entire assemblage, we observe a broad distribution of ages within each taphonomic grade (Fig. 5A). Interestingly, otoliths graded as pristine span almost the entire age range, in contrast to those of moderate, severe, and high taphonomic grade. Differences in taphonomic grade among groups are not significant (Kruskal Wallis test, $\chi^2 = 22.38$, $p = 0.049$). Otolith age correlates positively but weakly with mean alteration (Spearman rho = 0.25, $p = 0.026$). To factor out depth, a linear model, with the taphonomic score and depth as predictors and the $\log_{10}$-transformed age as response, suggests a significant relationship (slope of the taphonomic score $p = 0.0013$; slope of depth $p = 0.0003$; but note the low adjusted $R^2 = 0.22$). The results for the individual depths (Fig. 5B–D) show a significant, albeit weak, correlation between age and mean alteration only at 30 m (Spearman rho = 0.33, $p = 0.022$); at 10 and 40 m, there is no such correlation (Table 2) due to the very similar age ranges for the different taphonomic grades. In the 30 m station assemblage, otoliths from pelagic fishes show a monotonic increase of taphonomic damage with age (Spearman rho = 0.65, $p = 0.0005$; Fig. 5F), in striking contrast with demersal fishes, which show a negative nonsignificant correlation (Spearman rho = −0.37, $p = 0.09$; Fig. 5E).

Relationship between Postmortem Age and Alteration Variables.—A significant correlation between otolith alteration variables and age is found only in some cases (Table 2). Specifically, completeness is the variable that most commonly significantly correlates positively with age, followed by translucency, but the correlation coefficients are always ≤ 0.5. Even for individual alteration variables, the pristine grade encompasses a broad age range (Fig. 6 for the full dataset, Supplementary Figs. S1–S3 for each depth station). Nevertheless, for the otolith assemblage of the pelagic fishes at 30 m depth, all alteration variables positively and significantly correlate with age (Supplementary Figs. S4–S5).

Relationship between Postmortem Age and Multivariate Preservation.—Multivariate preservation does not differ among stations (PERMANOVA, $F = 0.768$, $p = 0.496$). The first PCoA axis

https://doi.org/10.1017/pab.2021.30 Published online by Cambridge University Press

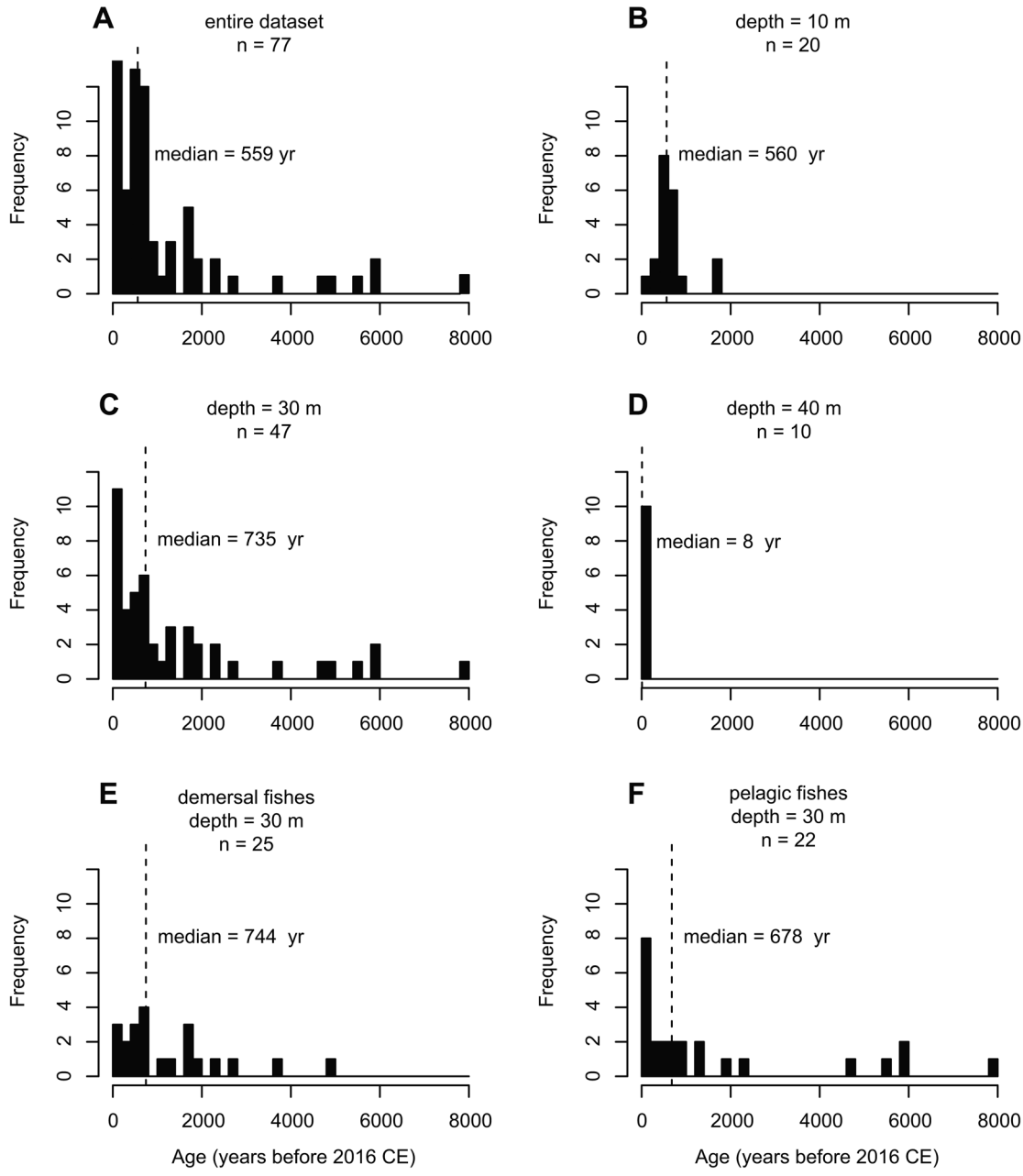


FIGURE 3. Otolith age–frequency distributions across a depth gradient on the Mediterranean southern Israeli shelf. The dashed lines indicate the median ages. A, Entire dataset; B–D, for the assemblages at 10, 30, and 40 m depths, respectively; E–F, only for the demersal and pelagic fishes, respectively, at 30 m depth.

explains 56% of the variation in otolith alteration of the full dataset and 78%, 60%, and 73% at 10, 30, and 40 m depths, respectively. For pelagic fishes at 30 m depth, the first PCoA axis explains 74% of the variation, but only 52% for the demersal fishes. This axis rarely orders otoliths according to their postmortem ages (Fig. 7). Accordingly, the Pearson correlation between the first PCoA axis and postmortem age is weak and nonsignificant (6). Again, the pelagic assemblage at 30 m depth shows the highest correlation and the

https://doi.org/10.1017/pab.2021.30 Published online by Cambridge University Press

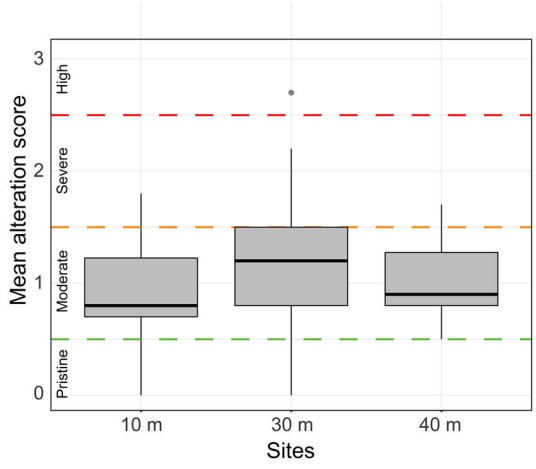


FIGURE 4. Mean taphonomic damage of the otoliths along the depth gradient. The distribution of the univariate taphonomic score does not differ among sites, but at the 40 m depth there is a lack of pristine otoliths, even though the death assemblage is very young.

p-value closest to 0.05. In the PCoAs with the best correlation between the first axis and postmortem age (full dataset and 30 m datasets; Fig. 7A,F), the vectors of the alteration variables increase along the first axis toward older otoliths. The correlation between the first PCoA axis and the individual alteration variables is strong (usually > to >> 0.5) and significant in most cases (Table 3). The first CAP axis reflects the increase in postmortem age (Fig. 8) with a weak relationship with most alteration variables. When adding water depth as a factor, age and depth diverge markedly, but most alteration variables (with the exception of translucency and completeness) show a greater relationship with age, suggesting that each sampled station represents a different taphofacies.

Discussion

The Taphonomic Clock Depends on the Taphofacies.—Local conditions (e.g., depth and type of sediment) are the major drivers of the strength of the taphonomic clock, as clearly shown by the different results at 30 and 40 m depths. At 30 m, the sedimentation rate is 0.2 mm/yr and the substrate is muddy sand, whereas at 40 m, the sedimentation rate is much higher, 2.4 mm/yr, and the substrate is muddy. The two depths are above and below the sand belt, respectively (today down to ~35 m depth), where fine-grained sediment originating from the Nile is transported northward along the Israeli coast (Hyams-Kaphzan et al. 2008; Avnaim-Katav et al. 2015). At 40 m, the otoliths look much altered, notwithstanding their very young age (4–174 yr). The same high alteration versus young age was observed for molluscan shells (Albano et al. 2020) and thus points to aggressive conditions in the sediments, possibly due to higher organic matter content and thus more acidic pore water. At the 30 m depth, the correlation between age and taphonomic grade is positive and significant, and particularly strong for pelagic fishes, for which individual alteration variables also correlate strongly with age (Table 2). In contrast, at 40 m, the correlation is positive but not significant. This latter result also derives from the combined high sedimentation rate and aggressive conditions, which lead to a very limited age range spanning only 170 yr. In such a short time frame, the stochastic processes of destruction and burial blur the taphonomic clock signal. In contrast, the otolith age range at 30 m spans most of the Holocene (6–7961 yr), enabling a clearer signal. The different taphonomic pathways caused by local conditions lead to distinct taphofacies (Brett and Baird 1986; Speyer and Brett 1986; Best and Kidwell 2000a; Tomašových and Zuschin 2009; Petró et al. 2018; Ritter et al. 2019). Importantly, variation in taphofacies may occur over relatively small spatial and depth scales, as in our case study.

The Taphonomic Clock Is Influenced by Organismal Life Histories.—In general, otolith input to seafloor sediments depends on fish production, as it is filtered through natural mortality and predation (Fig. 9A). For any given species, under constant fish production, a mass mortality event causes an increase in otolith input, whereas a change in its predator's abundance may cause a decrease or increase in otolith input depending on the type of predator. On one hand, variability in input rate generates age distributions that deviate from right-skewed exponential shapes, and unimodal distributions as observed at 10 or 30 m indicate a recent decline in input rate of otoliths. Thus, to explain differences between species in otolith input

https://doi.org/10.1017/pab.2021.30 Published online by Cambridge University Press

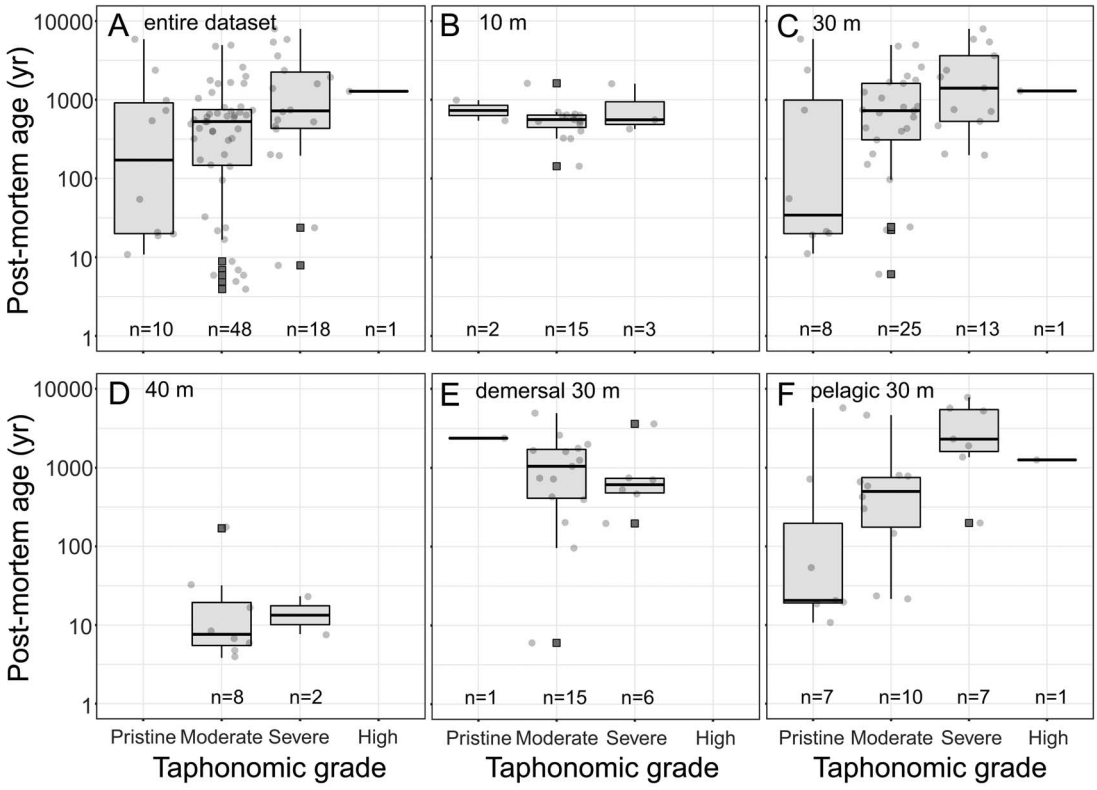


FIGURE 5. Box plots of postmortem age (log_{10}-transformed) vs. taphonomic alteration grade. A, Entire dataset; B–D, for the assemblages at 10, 30, and 40 m depths, respectively; E–F, only for the demersal and pelagic fishes, respectively, at 30 m depth. In most cases, young otoliths display the full range of taphonomic alteration, but at the 40 m depth, pristine otoliths are absent, notwithstanding the young age of the assemblage. A positive and significant correlation between taphonomic damage and age is observed only at the 30 m depth for pelagic fishes.

TABLE 2. Spearman correlation between alteration variables and age. Whereas this correlation is generally weak and nonsignificant, the taphonomic alteration of the otoliths of pelagic species at the 30 m depth correlates positively and significantly with postmortem age. Bold text indicates statistically significant values.

	Full dataset ($n = 77$)		−10 m ($n = 20$)		−30 m ($n = 47$)		−40 m ($n = 10$)		−30 m demersal ($n = 22$)		−30 m pelagic ($n = 25$)	
	rho	*p*	rho	*p*	rho	*p*	rho	*p*	rho	*p*	rho	*p*
Completeness	**0.38**	**0.0006**	0.33	0.14	**0.50**	**0.0002**	0.00	1	−0.12	0.59	**0.82**	**<<0.001**
Translucency	**0.25**	**0.03**	0.07	0.74	**0.33**	**0.02**	−0.18	0.60	−0.11	0.61	**0.57**	**0.002**
Bioerosion	0.38	0.10	−0.01	0.95	0.06	0.61	0.23	0.51	**−0.49**	**0.02**	**0.41**	**0.03**
Edge preservation	0.11	0.18	−0.17	0.44	0.22	0.12	0.50	0.13	−0.33	0.13	**0.50**	**0.009**
Dissolution	0.45	0.08	−0.31	0.17	0.24	0.10	0.26	0.46	−0.10	0.65	**0.42**	**0.03**
Ornamentation	0.34	0.10	−0.29	0.19	0.20	0.16	0.62	0.053	−0.22	0.31	**0.46**	**0.01**
Mean taphonomic grade	0.25	0.026	−0.15	0.54	**0.33**	**0.022**	0.52	0.12	−0.37	0.09	**0.65**	**0.0005**

trends over time, we must consider how the changes in the factors affecting fish production, natural mortality, and predation (temperature, oxygenation, substrate condition, depth) impact these species. On the other hand, disintegration and mixing affect the steepness of the age distributions, and these processes are controlled by depth, substrate, currents and waves, sedimentation rate, bioturbation, bioerosion, pore-water chemistry, temperature, and water oxygenation

https://doi.org/10.1017/pab.2021.30 Published online by Cambridge University Press

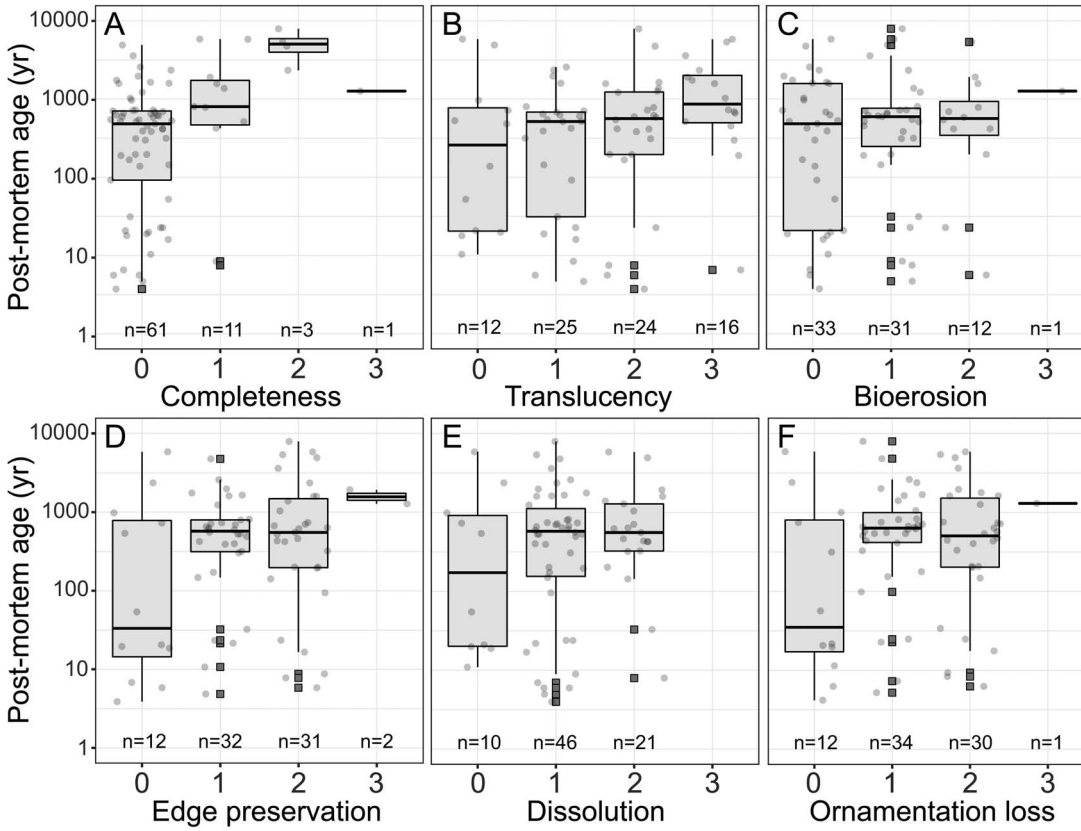


FIGURE 6. Box plots that show the distribution of ages (log_{10}-transformed) within alteration variable grades for the entire dataset, all depths pooled together. A, Completeness; B, translucency; C, bioerosion; D, edge preservation; E, dissolution; F, ornamentation loss. For all variables, pristine otoliths span a broad time range.

(Fig. 9B). Therefore, differences in the intrinsic properties of the otoliths of the compared species may result in one or more of these factors preferentially preserving/disintegrating and/or mixing the otoliths of one species. The final shape of the age distributions is a combined effect of input and preservation states (Tomašových et al. 2016). Consequently, apart from otolith inputs, we have to account for otolith intrinsic properties to estimate species temporal resolutions in otolith death assemblages.

Our investigation clearly shows that the taphonomic clock is influenced by the life histories of the target species, such as temporal variations in production and the fish lifestyle. At the 10 m depth, otolith ages range back to 1622 yr, but the abundance of the demersal species we dated shows a decline over the last few centuries, with no otoliths younger than 144 yr. Similarly, the otoliths of demersal fishes at 30 m span 6 to 4950 yr, but only a few of them are a few centuries old: only 2 (9%) of the dated otoliths are younger than 150 yr. The lack of young otoliths contrasts our expectation: taphonomic loss may follow different models, but all include a fast initial loss (e.g., exponential) that leads to typical right-skewed age–frequency distributions dominated by young otoliths, with a tail of few old ones (Tomašových et al. 2014, 2016; Albano et al. 2020). The relative rarity or absence of very young otoliths likely derives from smaller or absent input from the living assemblage (e.g., in Albano et al. 2016; Tomašových and Kidwell 2017; Tomašových et al. 2018), pointing to a decline of demersal species production at least locally (the 10 and 30 m stations are ~2.5 km apart). Interestingly, this decline cannot be observed

https://doi.org/10.1017/pab.2021.30 Published online by Cambridge University Press

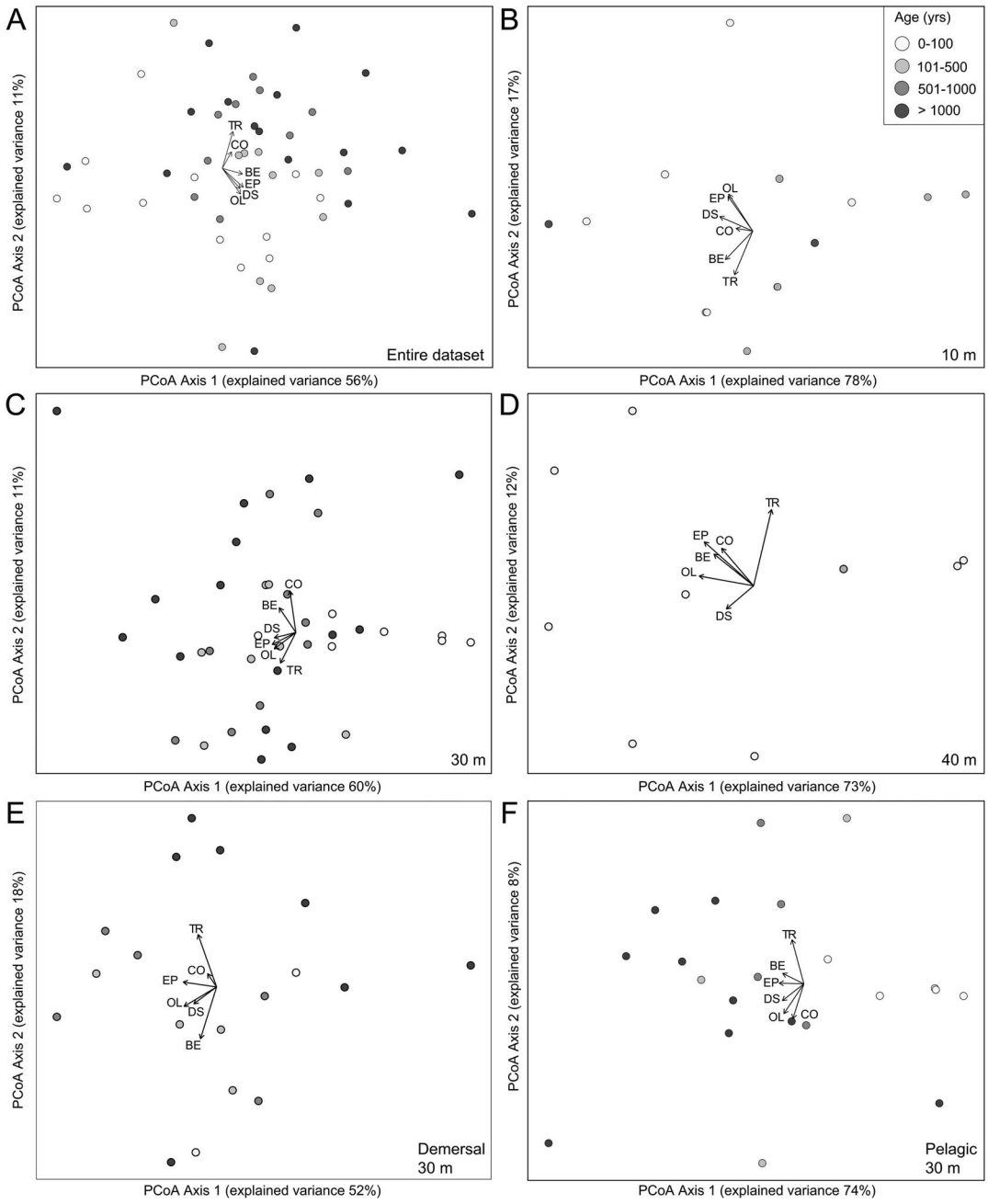


FIGURE 7. Principal coordinate analysis (PCoA) of alteration variables. The first PCoA axis hardly orders otoliths according to their postmortem age. Abbreviations: BE: bioerosion; CO: completeness; DS: dissolution; EP: edge preservation; OL: ornamentation loss; TR: translucency.

in the pelagic fishes we dated or in the infaunal bivalves *Donax semistriatus* and *Corbula gibba* at the same sites (Albano et al. 2020), suggesting that extrinsic taphonomic processes such as transport or preferential disintegration of demersal fish otoliths are unlikely. The lack of young otoliths at these depths implies that the assemblage lacks those most pristine, compacting the range of taphonomic damage to the altered end (only 2 [10%] and 1 [5%] otoliths

https://doi.org/10.1017/pab.2021.30 Published online by Cambridge University Press

TABLE 3. Correlation between principal coordinate analysis (PCoA) axis 1 and the alteration variables are strong and significant in most cases, suggesting that the first ordination axis orders otoliths according to taphonomic condition. Bold text indicates statistically significant values.

	Entire dataset	10 m	30 m	40 m	30 m demersal	30 m pelagic
Completeness	**0.43 ($p < 0.0001$)**	−0.38 ($p = 0.0997$)	**−0.41 ($p = 0.0048$)**	**−0.70 ($p = 0.0247$)**	−0.29 ($p = 0.1861$)	**−0.66 ($p = 0.0003$)**
Translucency	**0.66 ($p < 0.0001$)**	**−0.72 ($p = 0.0003$)**	**−0.77 ($p < 0.0001$)**	0.46 ($p = 0.177$)	**−0.70 ($p = 0.0003$)**	**−0.83 ($p < 0.0001$)**
Bioerosion	**0.79 ($p < 0.0001$)**	**−0.86 ($p < 0.0001$)**	**−0.74 ($p < 0.0001$)**	**−0.78 ($p = 0.0078$)**	−0.52 ($p = 0.0143$)	**−0.83 ($p < 0.0001$)**
Edge preservation	**0.87 ($p < 0.0001$)**	**−0.77 ($p < 0.0001$)**	**−0.90 ($p < 0.0001$)**	**−0.90 ($p = 0.0004$)**	**−0.80 ($p < 0.0001$)**	**−0.93 ($p < 0.0001$)**
Dissolution	**0.73 ($p < 0.0001$)**	**−0.90 ($p < 0.0001$)**	**−0.74 ($p < 0.0001$)**	−0.44 ($p = 0.2072$)	**−0.47 ($p = 0.0261$)**	**−0.86 ($p < 0.0001$)**
Ornamentation loss	**0.83 ($p < 0.0001$)**	**−0.80 ($p < 0.0001$)**	**−0.80 ($p < 0.0001$)**	**−0.92 ($p = 0.0001$)**	**−0.76 ($p < 0.0001$)**	**−0.90 ($p < 0.0001$)**

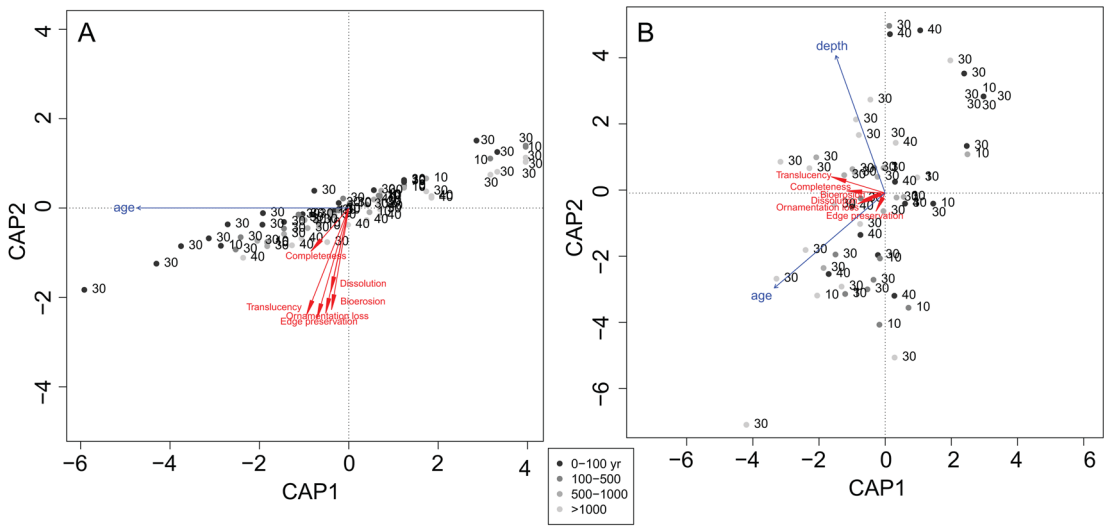


FIGURE 8. Constrained analysis of principal coordinates (CAP). A, CAP axis 1 reflects the increase in postmortem age, which has a weak relationship with most alteration variables. B, When the depth factor is added, alteration variables (with the exception of translucency and completeness) better align with age, suggesting that each station represents a different taphofacies.

were graded "pristine" at 10 m and for the demersal fish assemblage at 30 m, respectively, in contrast to 7 [28%] for the pelagic fish assemblage at 30 m; 5 [71%] of these are younger than 55 yr), thus hindering significant correlations.

The fish lifestyle (e.g., demersal vs. pelagic) may also influence postmortem processes. Predation is a significant cause of otolith input into the sediment, and predators differ between the two lifestyles: pelagic species such as the anchovies are preyed upon by pelagic and demersal fishes, whereas demersal species such as the gobies and the congrids are preyed upon by larger fishes and by fishes and seabirds, respectively (Froese and Pauly 2021). There is thus potential for differential out-of-habitat transport and alteration in the predators' digestive tracts (Jobling and Breiby 1986). The different results in terms of both direction and strength of the correlation between age and alteration variables between demersal (negative and nonsignificant) and pelagic (positive and significant) may point to such differences, but the bias introduced by the lack of young demersal fish otoliths hampers drawing any final conclusions.

https://doi.org/10.1017/pab.2021.30 Published online by Cambridge University Press

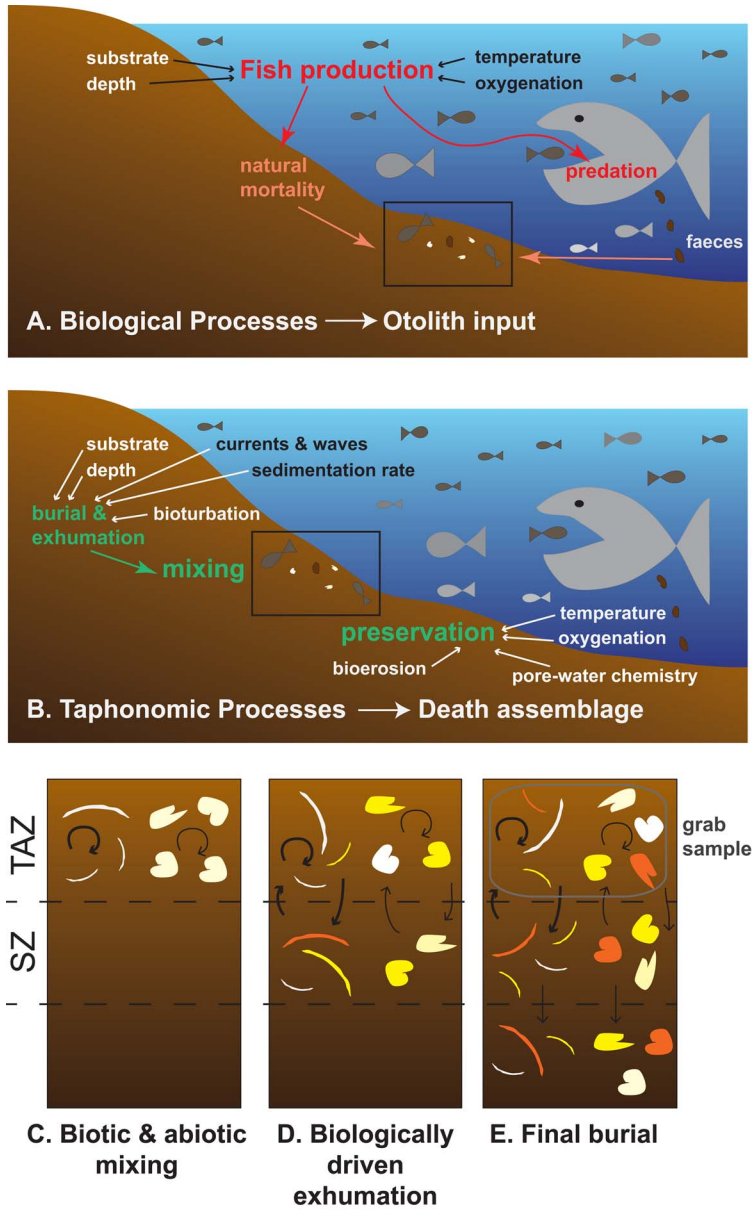


FIGURE 9. Simplified model showing the factors affecting the fate of otoliths from fish death to otolith final burial. A, Biological processes. Fish otoliths are deposited on the seafloor either after the decomposition of the fish carcass (natural mortality) or in predator feces (predation); the production of fish populations, which depends on temperature, substrate, water oxygenation, and depth, determines the rate of otolith input in the sediment. B–D, Taphonomic processes. Once at the sediment–water interface, otoliths are vulnerable to taphonomic damage, but they quickly get mixed into the surficial sediments (B). In the taphonomic active zone (TAZ), abiotic (temperature, oxygenation, and pore-water chemistry) and biotic (bioerosion) factors continue to affect otolith preservation/disintegration. In addition, they are mixed due to abiotic (currents and waves) and biotic (bioturbation) factors. Otoliths remain in the TAZ for periods comparable to those of similar-sized skeletal parts of other organisms, such as small bivalve shells (C). Otoliths get progressively deeper in the sediment and into the sequestration zone (SZ) at rates depending on sea bottom depth and sedimentation rate. In the SZ, loss occurs at a lower rate, and exhumation into the TAZ is still possible due to biological activity (e.g., of deep-burrowing invertebrates), contributing to further mixing and the occurrence of very old otoliths in the surficial death assemblage, which is retrieved from the TAZ with standard sampling methods such as Van Veen grabs (D). E, Fossilization. Once otoliths are buried deeper, they undergo diagenesis to form the fossil assemblage. For comparison (see "Discussion"), C–E also show how burial–exhumation affects bivalve shells. Otolith and bivalve colors (C–E) indicate the level of alteration (white: pristine; yellow: moderate; orange: strongly altered).

https://doi.org/10.1017/pab.2021.30 Published online by Cambridge University Press

Comparison with Other Taxa.—Taphonomic pathways, and thus the strength of the taphonomic clock, depend on local extrinsic factors for other taxa as well. For example, molluscan shells show different preservation states and correlation between preservation state and postmortem age in siliciclastic versus carbonate sediments (Kidwell et al. 2005). Carbonate areas in particular show a greater degree of biofoulers and more acidic pore waters, leading to a faster accrual of damage and eventually shell loss (Best and Kidwell 2000a,b; Kidwell et al. 2005). Consistently, brachiopod shells collected along a narrow and shallow depth gradient on a uniform mixed carbonate–siliciclastic shelf did not show significant differences in taphonomic patterns (Carroll et al. 2003). Still, we show here that even within homogenous shelves in terms of sediment type, the occurrence of organic-rich versus organic-poor sediments at relatively close distances may lead to different pore-water acidity and thus affect the preservation state and the strength of its correlation with age (like our stations at 30 and 40 m depths, which are 6 km apart on a siliciclastic shelf). Indeed, that taphonomic pathways depend on the environment of deposition is also a clear result of short-term taphonomic experiments (e.g., Callender et al. 2002; Powell et al. 2011).

Previous correlative studies based on Holocene–Recent molluscan shells in shallow shelves, thus similar to our own study, often showed only moderate correlation between preservation state and age (Powell and Davies 1990; Flessa et al. 1993; Kowalewski et al. 1994; Martin et al. 1996). In contrast, our case study shows that when an otolith death assemblage is not biased by strong variation in skeletal production or under particularly aggressive sediment conditions, preservation state and age strongly correlate positively (our results for pelagic species at the 30 m depth; Fig. 5F, Table 2, Supplementary Fig. S5). Under these conditions, the otolith taphonomic clock works predictably.

In contrast to molluscan shells that rapidly accrue damage, resulting in even young specimens appearing old, otoliths can be better preserved. At least some otoliths are deposited through predator feces (Martini 1965; Schwarzhans et al. 2018) (Fig. 9). Carnivorous fishes produce feces rich in calcium and phosphate, which can form an insoluble crystallic calcium phosphate matrix that increases their preservation potential (Hollocher and Hollocher 2012). Therefore, otoliths may be initially protected from degradation in the TAZ, further explaining why some old otoliths are still taphonomically pristine. The passage through the predator's digestive tract affects otoliths due to the stomach acids at a level depending on the kind of predator, the exposure time, and the otolith form and structure (Jobling and Breiby 1986). The residence time in the predator's digestive system is not expected to be sufficient for the complete disintegration of the otoliths. Instead, gastric acid may etch an otolith uniformly, without obliterating or enhancing its ornamentation, thus making it appear almost pristine, even though it has been somewhat reduced in size (Jobling and Breiby 1986).

These results suggest that testing the hypothesis of the taphonomic clock for any skeletal element requires a careful assessment of spatial heterogeneity in abiotic conditions and knowledge of the temporal population dynamics of the target species and its specific life histories.

Conclusions

Estimating the age of fossils and the temporal resolution of their assemblages is the first priority in all paleontological and paleobiological investigations. Our results indicate that the strength of the correlation between preservation state and postmortem age of fish otoliths depends on local extrinsic conditions, such as sediment type and pore-water acidity, as well as on the target species' life history. Nevertheless, in optimal conditions (i.e., chemically nonaggressive sediments, continuous species production), the taphonomic clock works predictably: old-looking otoliths in death assemblages recovered from shallow-marine shelves are likely to be old; broken, opaque, and largely dissolved or eroded otoliths can be safely regarded as old (≥1000 yr in our system), whereas pristine otoliths are unlikely to be old (older than 1000 yr here). Considering the present results, we suggest that future work should focus on evaluating the taphonomic

https://doi.org/10.1017/pab.2021.30 Published online by Cambridge University Press

clock hypothesis in different settings, particularly deeper marine as well as anoxic environments, where chemical processes may play a more dominant role.

Acknowledgments

This work was supported by the grants of the Austrian Science Fund (FWF) P28983-B29 "Historical Ecology of Lessepsian Migration" (PI: P.G.A.) and M2894-N "Deep-Time Climate Change Impact on Marine Food Webs" (PI: K.A.), and by the Palaeontological Association Research Grant "Time Resolution of Fish Death Assemblages on the Eastern Mediterranean Shelf," PA-RG201803 (to K.A.). This collaboration was facilitated by a Short-Term Scientific Mission funded by the COST Action CA15121 "Advancing Marine Conservation in the European and Contiguous Seas." The funders had no role in study design, data collection and analysis, decision to publish, or preparation of the manuscript. We thank S. Szidat for dating the *Bregmaceros* otoliths with the MICADAS method, B. S. Galil and M. Zuschin for useful discussion and support throughout the project, J. Steger for his help during sampling and material processing, and the three anonymous reviewers for their insightful comments.

Data Availability Statement

Data available from the Zenodo Digital Repository: https://doi.org/10.5281/zenodo.5147991.

References

Agiadi, K., and P. G. Albano. 2020. Holocene fish assemblages provide baseline data for the rapidly changing eastern Mediterranean. The Holocene 30:1438–1450.

Agiadi, K., M. Triantaphyllou, A. Girone, V. Karakitsios, and M. Dermitzakis. 2010. Paleobathymetric interpretation of the fish otoliths from the Lower–Middle Quaternary deposits of Kephallonia and Zakynthos Islands (Ionian Sea, western Greece). Rivista Italiana Di Paleontologia e Stratigrafia 116:63–78.

Agiadi, K., M. Triantaphyllou, A. Girone, and V. Karakitsios. 2011. The Early Quaternary palaeobiogeography of the eastern Ionian deep-sea teleost fauna: a novel palaeocirculation approach. Palaeogeography, Palaeoclimatology, Palaeoecology 306:228–242.

Agiadi, K., A. Antonarakou, G. Kontakiotis, N. Kafousia, P. Moissette, J.-J. Cornée, E. Manoutsoglou, and V. Karakitsios. 2017. Connectivity controls on the Late Miocene eastern Mediterranean fish fauna. International Journal of Earth Sciences 106:1147–1159.

Agiadi, K., A. Girone, E. Koskeridou, P. Moissette, J.-J. Cornée, and F. Quillévéré. 2018. Pleistocene marine fish invasions and paleoenvironmental reconstructions in the eastern Mediterranean. Quaternary Science Reviews 196:80–99.

Agiadi, K., C. Giamali, A. Girone, P. Moissette, E. Koskeridou, and V. Karakitsios. 2020. The Zanclean marine fish fauna and palaeoenvironmental reconstruction of a coastal marine setting in the eastern Mediterranean. Palaeobiodiversity and Palaeoenvironments 100:773–792.

Aguilera, O., W. Schwarzhans, H. Moraes-Santos, and A. Nepomuceno. 2014. Before the flood: Miocene Otoliths from eastern Amazon Pirabas Formation reveal a Caribbean-type fish fauna. Journal of South American Earth Sciences 56:422–446.

Albano, P. G. 2014. Comparison between death and living land mollusk assemblages in six forested habitats in northern Italy. Palaios 29:338–347.

Albano, P. G., and B. Sabelli. 2011. Comparison between death and living molluscs assemblages in a Mediterranean infralittoral offshore reef. Palaeogeography, Palaeoclimatology, Palaeoecology 310:206–215.

Albano, P. G., N. Filippova, J. Steger, D. S. Kaufman, A. Tomašových, M. Stachowitsch, and M. Zuschin. 2016. Oil platforms in the Persian (Arabian) Gulf: living and death assemblages reveal no effects. Continental Shelf Research 121:21–34.

Albano, P. G., Q. Hua, D. Kaufman, A. Tomašových, M. Zuschin, and K. Agiadi. 2020. Radiocarbon dating supports bivalve-fish age coupling along a bathymetric gradient in high-resolution paleoenvironmental studies. Geology 48:589–593.

Allen, A. P., M. A. Kosnik, and D. S. Kaufman. 2013. Characterizing the dynamics of amino acid racemization using time-dependent reaction kinetics: a Bayesian approach to fitting age-calibration models. Quaternary Geochronology 18:63–77.

Anderson, M. J., and T. J. Willis. 2003. Canonical analysis of principal coordinates: a useful method of constrained ordination for ecology. Ecology 84:511–525.

Andrus, C. F. T., D. E. Crowe, D. H. Sandweiss, E. J. Reitz, and C. S. Romanek. 2002. Otolith $\Delta^{18}O$ record of mid-Holocene sea surface temperatures in Peru. Science 295:1508–1511.

Avnaim-Katav, S., O. Hyams-Kaphzan, Y. Milker, and A. Almogi-Labin. 2015. Bathymetric zonation of modern shelf benthic foraminifera in the Levantine basin, eastern Mediterranean Sea. Journal of Sea Research 99:97–106.

Belanger, C. L. 2011. Evaluating taphonomic bias of paleoecological data in fossil benthic foraminiferal assemblages. Palaios 26:767–778.

Bertucci, T., O. Aguilera, C. Vasconcelos, G. Nascimento, G. Marques, K. Macario, C. Queiroz de Albuquerque, T. Lima, and A. Belém. 2018. Late Holocene palaeotemperatures and palaeoenvironments in the southeastern Brazilian coast inferred from otolith geochemistry. Palaeogeography, Palaeoclimatology, Palaeoecology 503:40–50.

Best, M. M. R., and S. M. Kidwell. 2000a. Bivalve taphonomy in tropical mixed siliciclastic-carbonate settings. I. Environmental variation in shell condition. Paleobiology 26:80–102.

Best, M. M. R., and S. M. Kidwell. 2000b. Bivalve taphonomy in tropical mixed siliciclastic-carbonate settings. II. Effect of bivalve life habits and shell types. Paleobiology 26:103–115.

Brett, C. E., and G. C. Baird. 1986. Comparative taphonomy; a key to paleoenvironmental interpretation based on fossil preservation. Palaios 1:207–227.

Bright, J., D. Kaufman, K. E. Whitacre, C. Ebert, J. R. Southon, P. G. Albano, C. Flores, T. K. Frazer, Q. Hua, M. Kowalewski, J. C. Martinelli, D. Oakley, W. G. Parker, M. Retelle, M. N. Ritter, M. M Rivadeneira, D. Scarponi, Y. Yares, M. Zuschin, and D. S. Kaufman. 2021. comparing rapid and standard ^{14}C ages from an Assortment of Biogenic carbonates. Radiocarbon 63:387–403.

Bush, S. L., G. M. Santos, X. Xu, J. R. Southon, N. Thiagarajan, S. K. Hines, and J. F. Adkins. 2013. Simple, rapid, and cost effective: a screening method for ^{14}C analysis of small carbonate samples. Radiocarbon 55:631–640.

Callender, W. R., E. N. Powell, and G. M. Staff. 1994. Taphonomic rates of molluscan shells placed in autochthonous assemblages on the Louisiana continental slope. Palaios 9:60–73.

https://doi.org/10.1017/pab.2021.30 Published online by Cambridge University Press

Callender, W. R., G. M. Staff, K. M. Parsons-Hubbard, E. N. Powell, G. T. Rowe, S. E. Walker, C. E. Brett, A. Raymond, D. D. Carlson, S. White, and E. A. Heise. 2002. Taphonomic trends along a fore-reef slope: Lee Stocking Island, Bahamas. I. Location and water depth. Palaios 17:50–65.

Carroll, M., M. Kowalewski, M. G. Simões, and G. A. Goodfriend. 2003. Quantitative estimates of time-averaging in terebratulid brachiopod shell accumulations from a modern tropical shelf. Paleobiology 29:381–402.

Cernohorsky, N. H., M. Horsak, and R. D. Cameron. 2010. Land snail species richness and abundance at small scales: the effects of distinguishing between live individuals and empty shells. Journal of Conchology 40:233.

Cristini, P. A., and C. G. De Francesco. 2019. Taphonomic field experiment in a freshwater shallow lake: alteration of gastropod shells below the sediment–water interface. Journal of Molluscan Studies 85:404–413.

Degens, E. T., W. G. Deuser, and R. L. Haedrich. 1969. Molecular structure and composition of fish otoliths. Marine Biology 2:105–113.

Flessa, K. W. 1993. Time-averaging and temporal resolution in Recent marine shelly faunas. Short Courses in Paleontology 6:9–33.

Flessa, K. W., A. H. Cutler, and K. H. Meldahl. 1993. Time and taphonomy: quantitative estimates of time-averaging and stratigraphic disorder in a shallow marine habitat. Paleobiology 19:266–286.

Frey, R. W., and J. D. Howard. 1986. Taphonomic characteristics of offshore mollusk shells, Sapelo Island, Georgia. Tulane Studies in Geology and Paleontology 19. https://journals.tulane.edu/tsgp/article/view/1054.

Froese, R., and D. Pauly, eds. 2021. FishBase. www.fishbase.org, version 02/2021.

Girone, A. 2005. Response of otolith assemblages to sea-level fluctuations at the lower Pleistocene Montalbano Jonico Section (southern Italy). Bolletino della Societa Paleontologica Italiana 44:35–45.

Girone, A., D. Nolf, and H. Cappetta. 2006. Pleistocene fish otoliths from the Mediterranean basin: a synthesis. Geobios 39:651–671.

Golik, A. 1993. Indirect evidence for sediment transport on the continental shelf off Israel. Geo-Marine Letters 13:159–164.

Goodman-Tchernov, B. N., H. W. Dey, E. G. Reinhardt, F. McCoy, and Y. Mart. 2009. Tsunami waves generated by the Santorini eruption reached eastern Mediterranean shores. Geology 37:943–946.

Gottschalk, J., S. Szidat, E. Michel, A. Mazaud, G. Salazar, M. Battaglia, J. Lippold, and S. L. Jaccard. 2018. Radiocarbon measurements of small-size foraminiferal samples with the mini carbon dating system (MICADAS) at the University of Bern: implications for paleoclimate reconstructions. Radiocarbon 60:469–491.

Harnik, P. G., M. L. Torstenson, and M. A. Williams. 2017. Assessing the effects of anthropogenic eutrophication on marine bivalve life history in the northern Gulf of Mexico. Palaios 32:678–688.

Hassan, G. S., E. Tietze, P. A. Cristini, and C. G. De Francesco. 2014. Differential preservation of freshwater diatoms and mollusks in Late Holocene sediments: paleoenvironmental implications. Palaios 29:612–623.

Henderson, S. W., and R. W. Frey. 1986. Taphonomic redistribution of mollusk shells in a tidal inlet channel, Sapelo Island, Georgia. Palaios 1:3–16.

Hollocher, K., and T. C. Hollocher. 2012. Early process in the fossilization of terrestrial feces to coprolites, and microstructure preservation. *In*: Vertebrate Coprolites. Bulletin of the New Mexico Museum of Natural History and Science 57:79–92. Albuquerque: New Mexico Museum of Natural History & Science.

Hyams-Kaphzan, O., A. Almogi-Labin, D. Sivan, and C. Benjamini. 2008. Benthic foraminifera assemblage change along the southeastern Mediterranean inner shelf due to fall-off of Nile-derived siliciclastics. Neues Jahrbuch für Geologie und Paläontologie - Abhandlungen 248:315–344.

Inman, D. L., and S. A. Jenkins. 1984. The Nile littoral cell and man's impact on the coastal zone of the southeastern Mediterranean. Pp. 1600–1617 *in* 19th International Conference on Coastal Engineering, Houston, Tex. https://doi.org/10.1061/9780872624382.110.

Jobling, M., and A. Breiby. 1986. The use and abuse of fish otoliths in studies of feeding habits of marine piscivores. Sarsia 71:265–274.

Jones, W. A., and D. M. Checkley. 2019. Mesopelagic fishes dominate otolith record of past two millennia in the Santa Barbara basin. Nature Communications 10:4564.

Kidwell, S. M. 1993. Patterns of time-averaging in the shallow marine fossil record. Short Courses in Paleontology 6:275–300.

Kidwell, S. M. 1998. Time-averaging in the marine fossil record: overview of strategies and uncertainties. Geobios 30:977–995.

Kidwell, S. M., M. M. R. Best, and D. S. Kaufman. 2005. Taphonomic trade-offs in tropical marine death assemblages: differential time averaging, shell loss, and probable bias in siliciclastic vs. carbonate facies. Geology 33:729–732.

Klompmaker, A. A., R. W. Portell, and M. G. Frick. 2017. Comparative experimental taphonomy of eight marine arthropods indicates distinct differences in preservation potential. Palaeontology 60:773–794.

Kowalewski, M., K. W. Flessa, and J. A. Aggen. 1994. Taphofacies analysis of recent shelly cheniers (beach ridges), northeastern Baja California, Mexico. Facies 31:209.

Kowalewski, M., G. A. Goodfriend, and K. W. Flessa. 1998. High-resolution estimates of temporal mixing within shell beds: the evils and virtues of time-averaging. Paleobiology 24:287–304.

Landini, W., and C. Sorbini. 2005. Evolutionary trends in the Plio-Pleistocene ichthyofauna of the Mediterranean basin: nature, timing and magnitude of the extinction events. Quaternary International 131:101–107.

Lin, C. H., B. de Garcia, M. E. R. Pierotti, A. H. Andrews, K. Griswold, A. O'Dea. 2019. Reconstructing reef fish communities using fish otoliths in coral reef sediments. PLoS ONE 14:e0218413.

Martin, R. E., J. F. Wehmiller, M. S. Harris, and W. D. Liddell. 1996. Comparative taphonomy of bivalves and foraminifera from Holocene tidal flat sediments, Bahia La Choya, Sonora, Mexico (northern Gulf of California): taphonomic grades and temporal resolution. Paleobiology 22:80–90.

Martini, E. 1965. Die Fischfauna von Sieblos/Rhön (Oligozän). Senckenbergiana Lethaea 46:291–314.

Oksanen, J., F. G. Blanchet, M. Friendly, R. Kindt, P. Legendre, D. McGlinn, P. R. Minchin, R.B. O'Hara, G. L. Simpson, P. Solymos, M. H. H Stevens, E. Szoecs, and H. Wagner. 2015. Vegan: community ecology package. https://cran.r-project.org/web/packages/vegan, accessed 10 February 2021.

Olszewski, T. D. 2004. Modeling the influence of taphonomic destruction, reworking, and burial on time-averaging in fossil accumulations. Palaios 19:39–50.

Petró, S. M., M. N. Ritter, M. A. Gómez Pivel, and J. C. Coimbra. 2018. Surviving in the water column: defining the taphonomically active zone in pelagic systems. Palaios 33:85–93.

Powell, E. N., and D. J. Davies. 1990. When is an "old" shell really old? Journal of Geology 98:823–844.

Powell, E. N., K. M. Parsons-Hubbard, W. R. Callender, G. M. Staff, G. T. Rowe, C. E. Brett, S. E. Walker, A. Raymond, D. D. Carlson, S. White, and E. A. Heise. 2002. Taphonomy on the continental shelf and slope: two-year trends—Gulf of Mexico and Bahamas. Palaeogeography, Palaeoclimatology, Palaeoecology 184:1–35.

Powell, E. N., W. R. Callender, G. M. Staff, K. M. Parsons-Hubbard, C. E. Brett, S. E. Walker, A. Raymond, and K. A. Ashton-Alcox. 2008. Molluscan shell condition after eight years on the sea floor—taphonomy in the Gulf of Mexico and Bahamas. Journal of Shellfish Research 27:191–225.

Powell, E. N., G. M. Staff, W. R. Callender, K. A. Ashton-Alcox, C.. E. Brett, K. M. Parsons-Hubbard, S. E. Walker, and A. Raymond. 2011. Taphonomic degradation of molluscan remains during

https://doi.org/10.1017/pab.2021.30 Published online by Cambridge University Press

thirteen years on the continental shelf and slope of the northwestern Gulf of Mexico. Palaeogeography, Palaeoclimatology, Palaeoecology 312:209–232.

Price, G. D., D. Wilkinson, M. B. Hart, K. N. Page, and S. T. Grimes. 2009. Isotopic analysis of coexisting Late Jurassic fish otoliths and molluscs: implications for upper-ocean water temperature estimates. Geology 37:215–218.

R Development Core Team. 2019. R: a language and environment for statistical computing. Vienna, Austria: R Foundation for Statistical Computing.

Ritter, M. N., F. Erthal, M. A. Kosnik, J. C. Coimbra, and D. S. Kaufman. 2017. Spatial variation in the temporal resolution of subtropical shallow-water molluscan death assemblages. Palaios 32:572–583.

Ritter, M. N., F. Erthal, and J. C. Coimbra. 2019. Depth as an overarching environmental variable modulating preservation potential and temporal resolution of shelly taphofacies. Lethaia 52:44–56.

Sandweiss, D. H., C. F. T. Andrus, A. R. Kelley, K. A. Maasch, E. J. Reitz, and P. B. Roscoe. 2020. Archaeological climate proxies and the complexities of reconstructing Holocene El Niño in coastal Peru. Proceedings of the National Academy of Sciences USA 117:8271–8279.

Schulz-Mirbach, T., M. Olbinado, A. Rack, A. Mittone, A. Bravin, R. R. Melzer, F. Ladich, and M. Heß. 2018. In-situ visualization of sound-induced otolith motion using hard X-ray phase contrast imaging. Scientific Reports 8:3121.

Schwarzhans, W. W., T. D. Murphy, and M. Frese. 2018. Otoliths in situ in the stem teleost *Cavenderichthys talbragarensis* (Woodward, 1895), otoliths in coprolites, and isolated otoliths from the Upper Jurassic of Talbragar, New South Wales, Australia. Journal of Vertebrate Paleontology 38:e1539740.

Schwarzhans, W., K. Agiadi, and G. Carnevale. 2020. Late Miocene–Early Pliocene evolution of Mediterranean gobies and their environmental and biogeographic significance. Rivista Italiana di Paleontologia e Stratigrafia 126:657–724.

Speyer, S. E., and C. E. Brett. 1986. Trilobite taphonomy and Middle Devonian taphofacies. Palaios 1:312–327.

Tomašových, A., and S. M. Kidwell. 2017. Nineteenth-century collapse of a benthic marine ecosystem on the open continental shelf. Proceedings of the Royal Society of London B 284:20170328.

Tomašových, A., and M. Zuschin. 2009. Variation in brachiopod preservation along a carbonate shelf-basin transect (Red Sea and Gulf of Aden): environmental sensitivity of taphofacies. Palaios 24:697–716.

Tomašových, A., S. M. Kidwell, R. F. Barber, and D. S. Kaufman. 2014. Long-term accumulation of carbonate shells reflects a 100-fold drop in loss rate. Geology 42:819–822.

Tomašových, A., S. M. Kidwell, and R. F. Barber. 2016. Inferring skeletal production from time-averaged assemblages: skeletal loss pulls the timing of production pulses towards the modern period. Paleobiology 42:54–76.

Tomašových, A., J. Schlogl, A. Biron, N. Hudackova, and T. Mikus. 2017. Taphonomic clock and bathymetric dependence of cephalopod preservation in bathyal, sediment-starved environments. Palaios 32:135–152.

Tomašových, A., I. Gallmetzer, A. Haselmair, D. S. Kaufman, M. Kralj, D. Cassin, R. Zonta, and M. Zuschin. 2018. Tracing the effects of eutrophication on molluscan communities in sediment cores: outbreaks of an opportunistic species coincide with reduced bioturbation and high frequency of hypoxia in the Adriatic Sea. Paleobiology 44:575–602.

Wehmiller, J. F., L. L. York, and M. L. Bart. 1995. Amino acid racemization geochronology of reworked Quaternary mollusks on U.S. Atlantic coast beaches: implications for chronostratigraphy, taphonomy, and coastal sediment transport. Marine Geology 124:303–337.

Yanes, Y. 2012. Shell taphonomy and fidelity of living, dead, Holocene, and Pleistocene land snail assemblages. Palaios 27:127–136.

https://doi.org/10.1017/pab.2021.30 Published online by Cambridge University Press